Mail Delivery Path Optimization

ME4 B08502022 白為霖 ME4 B08502076 胡鈞傑 ME4 B08502091 葉逢恩

I. Background

We are designing an automated mail delivery robotic arm, whose task is to deliver mail into a mailbox. The robotic arm targets the mailbox and moves toward the baffle.

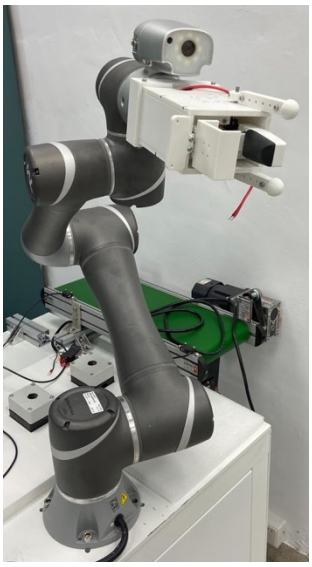

Figure (1). Gripper on the robotic arm

When the arm is sending the mail into the box, it will push the mail through the baffle, where the mail will be bent by a moment from the torsion spring and the corresponding friction force on the surface would also cause deflection. The resulting stress will cause deflection on the mail. Thus, our optimization problem is to select a path that minimizes the deflection, so that the mail will not be damaged during the process.

II. Literature Review

The path planning is determined by the deflection of mails, so we put our focus on the material property of paper.

Compared with other materials, i.e. metal, paper and paperboard exhibit complex mechanical behaviors, commonly characterized by a highly anisotropic linear elastic response under moderate mechanical loading and non-linear plastic response under high loading. In the optimization process, we assume the mail is under moderate mechanical loading, and we still have to develop the correct formula for deflection (strain).

Paper I. Orthotropic elastic–plastic material model for paper materials [1]

The mechanical response of machine-made paper is highly dependent on the loading direction, i.e. machine-made paper is an anisotropic material. Independently of the loading situation, the mechanical behavior of paper is largely dependent on the fiber shapes, the bond density, and the properties of the bonds. Furthermore, the fiber orientation and the longitudinal properties of the fibers are important factors contributing to the in-plane behavior of paper, while the out-of-plane behavior of paper instead is largely dependent on properties perpendicular to the longitudinal direction. The differences in mechanisms governing the in-plane and out-of-plane behavior of paper make three-axial continuum modelling of paper highly complex.

A simplifying and accurate treatment of the anisotropy of paper was made possible by the assumption of orthotropy, meaning that the material exhibits three mutually orthogonal planes of symmetry. These three principal material directions of machine-made paper commonly coincide with the MD, the cross-machine direction (CD) and the thickness direction (ZD), as indicated in figure (2). However, in this optimization problem, we simplify the paper model by supposing the mail is only affected by forces in MD direction, which may cause the out-of-plane behaviors of the paper.

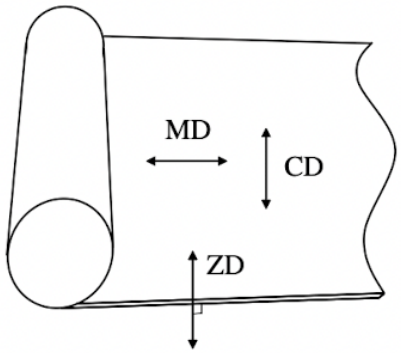

Figure (2). Principle materials direction of paper

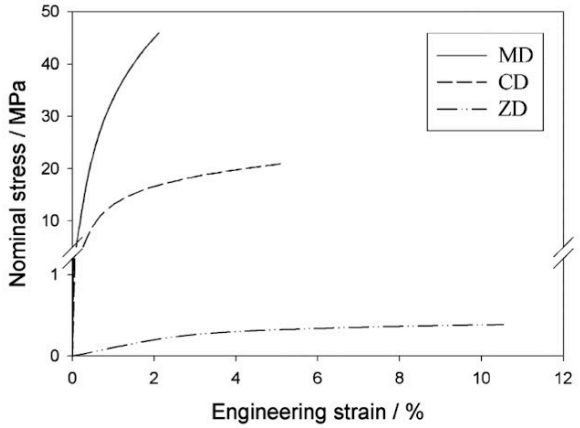

Figure (3). Material behavior in the principal material directions of a paperboard

Unloading from some point on the non-linear part of the stress–strain curve further results in a permanent deformation and the stiffness under unloading generally coincides well with the elastic modulus. The uniaxial behavior in the principal material directions of most paper grades under strictly increased loading is well described by the Ramberg–Osgood relation, which is specialized at describing the nonlinear relationship between stress and strain in materials near their yield point. The uniaxial Ramberg–Osgood form (1943) in slightly modified form is given by

$$\varepsilon = \frac{\sigma}{E} + \left(\frac{\sigma}{E_0}\right)^n \tag{1}$$

where σ is the uniaxial stress, ε is the corresponding strain, E is Young's modulus and E_0 and n are the hardening modulus and the hardening exponent, respectively.

Paper II. Advanced metal-forming technologies for automotive applications [2]

The work hardening exponent, n, of a material is a measure for how quickly the material gains strength when it is being deformed. The hardening exponent, n, can be obtained from the slope of the true stress versus true strain curve in a tensile test, plotted on a logarithmic scale (see figure (4)). The relationship between stress and strain can be expressed in an equation:

$$\sigma = k\varepsilon^n \tag{2}$$

where σ and ε are the true stress and strain and k and n are constants.

Thus, we can calculate n by:

$$n = \frac{\log(\sigma)}{\log(\varepsilon)} \tag{3}$$

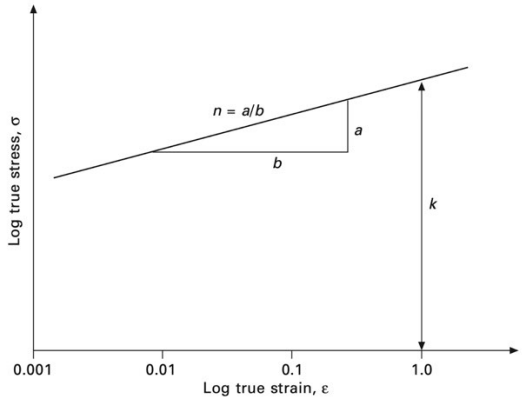

Figure (4). Logarithmic representation of true stress-strain curve with n the work hardening exponent

After the investigation of the material property of paper, we may successfully set the deflection of mails as the objective function for path planning. For industrial development, path planning can be operated with a camera for obstacle avoidance, and it can further accomplish Human-robot collaboration in industrial environment.

III. Problem Formulation

Paper Model

In our project, we select Kraft Paper as the tested sample. According to figure (5), elastic modulus E=3470 MPa in the MD direction, and refer to the result of *Paper I.*, hardening modulus E0=176.2 MPa (figure (6)).

To get the hardening exponent, we transferred σ-ε (figure (7)) into log(σ) - log(ε) during the forming process, and calculate the slope n = 0.58 in figure (8).

	Newsprint		Kraft paper		Board I		Board II	
Basis weight, g/m^2	45		70		120		240	
Thickness, μm	72		100		154		390	
Density, kg/m^3	643		700		779		620	
	MD	CD	MD	CD	MD	CD	MD	CD
Elastic modulus, MPa	4560	873	3470	2520	6780	3570	5420	1900
Tensile strength, MPa	31.9	10.8	57.3	33.1	57.7	37.4	45.0	15.0
Failure strain, %	0.92	2.8	5.4	6.5	2.6	6.0	1.3	5.1
Fracture energy, kJ/m^2	7.10	4.52	29.0	24.6	17.0	18.5	14.8	14.2

Figure (5). Property of different kinds of paper

Model	N	E_0/MPa	A	B	C	D	k
Quadratic	4.3224	176.2	1	2.441	2.441	1.384	1
Non-quadratic	4.3224	176.2	1	2.534	2.534	1.395	0.680

Figure (6). Hardening modulus under two different models

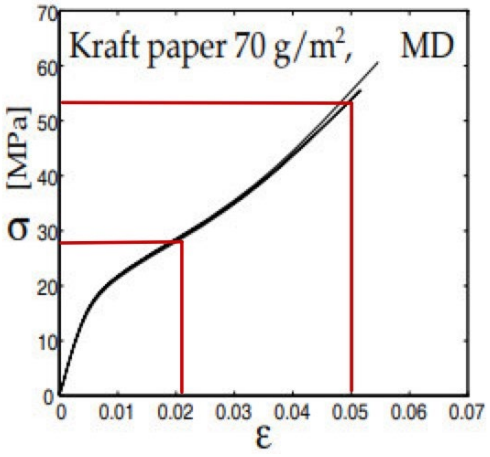

Figure (7). σ-ε (Kraft Paper)

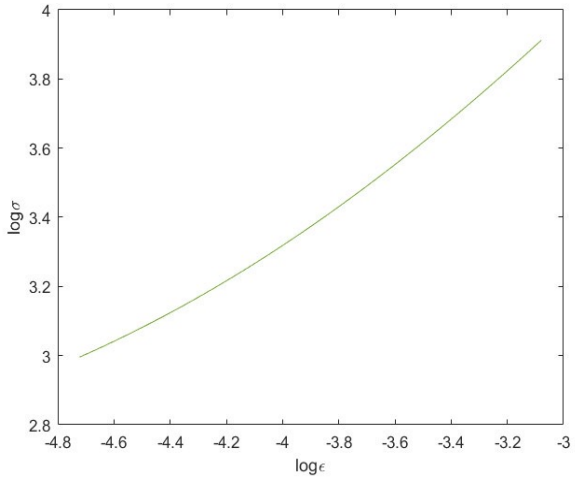

Figure (8). log(σ) -log(ε) (Kraft Paper)

Scenario Formulation

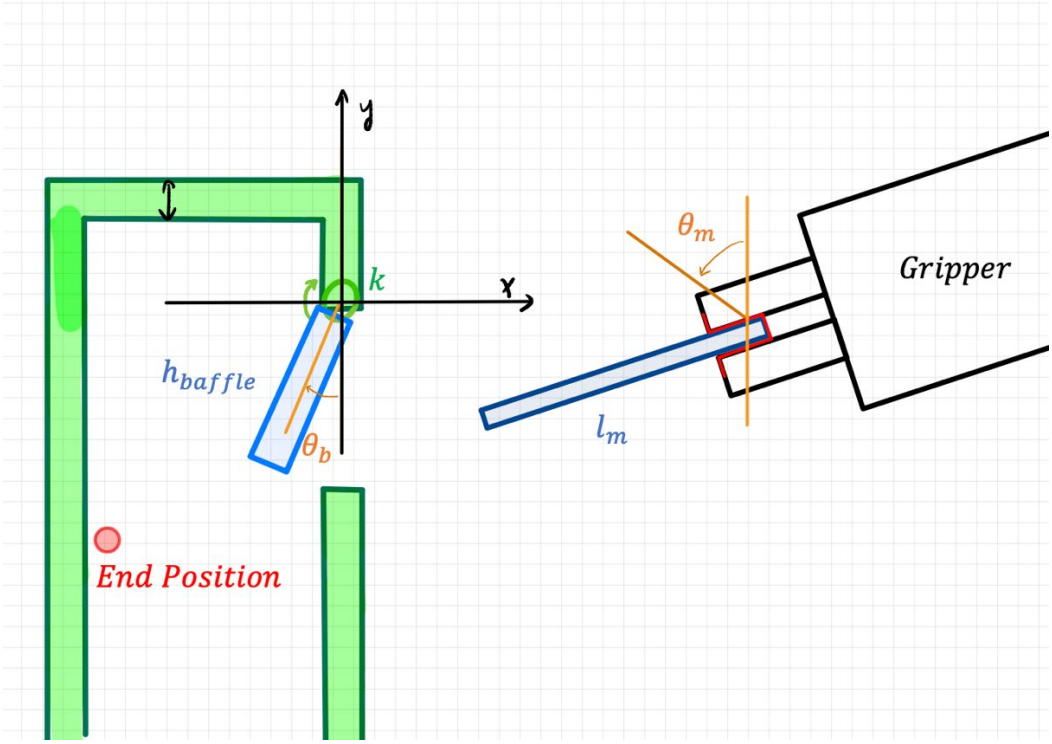

Figure (9). Schematic diagram for the whole model

The mail delivery maneuver is assumed as a 2-D motion in our scenario. During the mail delivery, the baffle of the mailbox will have contact with the mail and thus cause deformation of the mail. To prevent the mail from being severely wrinkled, we must optimize the path of the delivery. Aiming to minimize the deformation, our objective function is selected as the average strain ε_{avg} of the mail in the MD direction during the delivery.

$$f(x) = \varepsilon_{avg} = \frac{\sum_{i=1}^{N_b} \varepsilon_i}{N_b} \quad , N_b = number\ of\ selected\ point\ on\ bezier\ curve \qquad (4)$$

Parameters

$Mail\ size:\ (length, width, thickness) = (225\ mm, 125\ mm, 0.4\ mm)$

$Mailbox\ size: (w_m, d_m, h_m) = (200\ mm, 100\ mm, 260\ mm)$ [3]

$Baffle\ size:\ (w_b, h_b) = (140mm, 15mm)$ [3]

$Baffle\ weight:\ m_b = 38\ g$ [3]
$Torsion\ spring\ constant:\ k = 0.0289\ Nm$ [4]

$Friction\ coefficient\ between\ paper\ and\ steel: \mu = 0.4$ [5]

$Cross\ sectional\ area: A = 0.125 * (0.4E - 6) * N\ \ mm^2$
$Elastic\ modulus:\ E1 = 3470 * 10^6\ Pa$ [1]
$Hardening\ modulus: E0 = 176.2 * 10^6\ Pa$ [1]
$Gravitational\ acceleration:\ g = 9.81\ m/s^2$

Variable

$Number\ of\ paper\ in\ one\ stack: N$
$Number\ of\ selected\ point\ on\ bezier\ curve: N_b$
$Point\ for\ cubic\ bezier\ curve: P_0, P_1, P_2, P_2$

Statics

The baffle is simplified as a 1-DOF pendulum jointed with rotating shaft through a torsion spring.

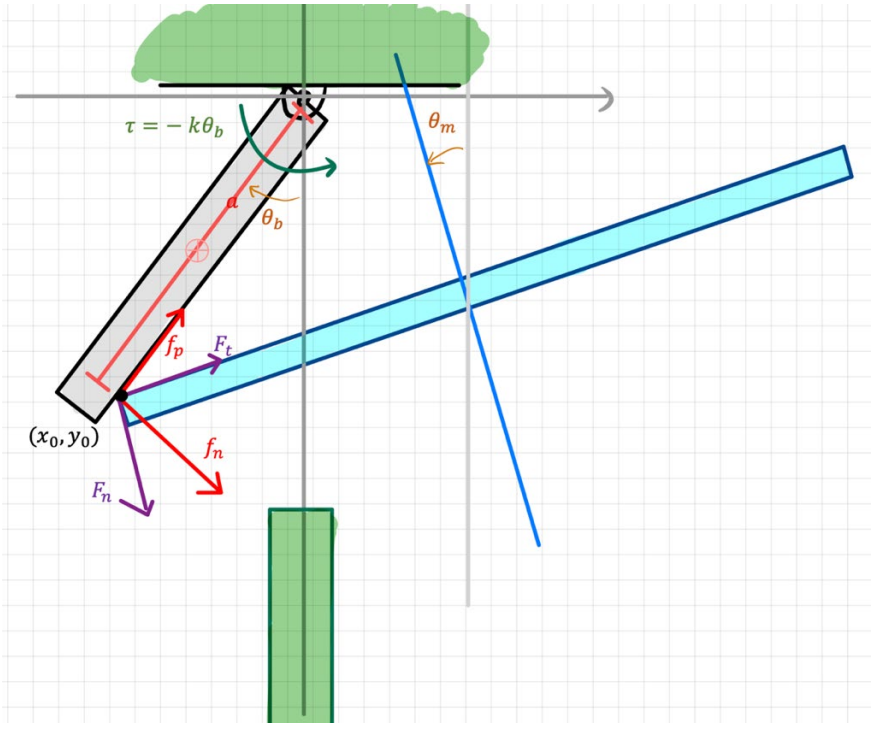

Figure (10). Schematic diagram 1 for the static model

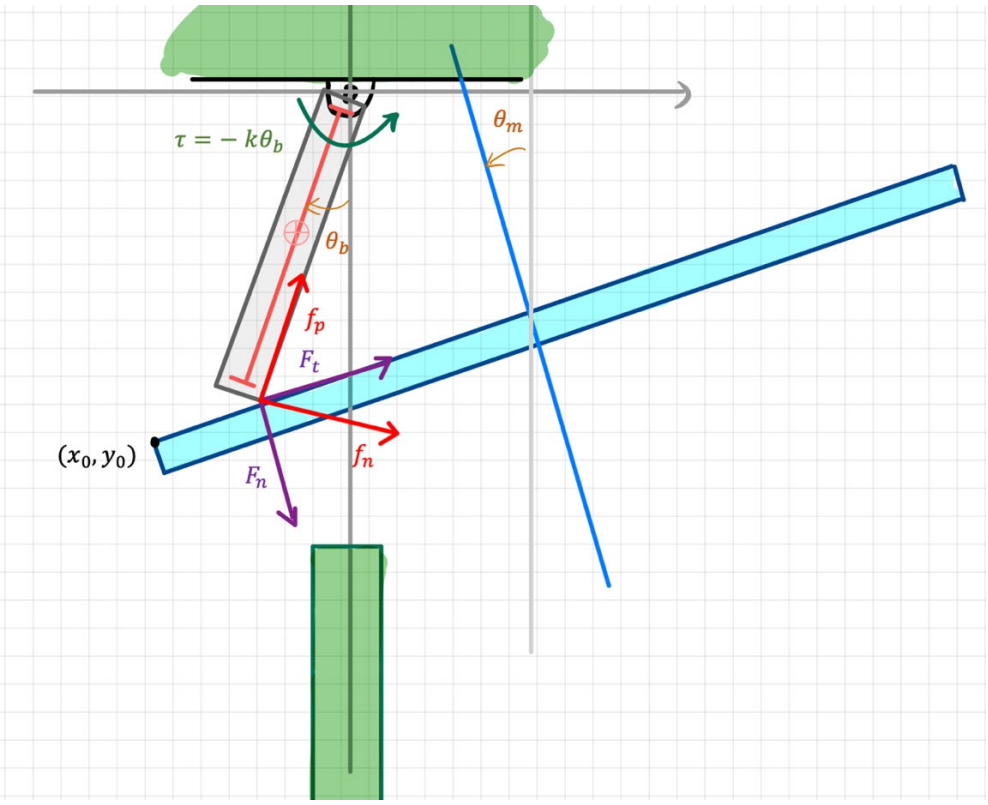

Figure (11). Schematic diagram 2 for the static model

To calculate the deformation, we need to analyze the contact force between baffle and mail. The dynamic of the system is analyzed by equation

$$J\,\theta_b'' \;=\; -0.5 * mgh_b sin\theta_b \;+ f_n \;* a - k * \theta_b \tag{5}$$

As we assume every moment it will be a static system, the normal force f_n the mail apply on the baffle will be:

$$f_n \;= \frac{k * \theta_b + 0.5 * mgh_b sin\theta_b}{a} \tag{6}$$

The friction force between the baffle and mail will be:

$$f_p \;= \mu * f_n \tag{7}$$

$$a \;=\; min(\sqrt{x_o{}^2 \;+\; y_o{}^2}\,, h\_b\,) \tag{8}$$

To decide θ_b, we need to consider two situations, one is where the head of the mail is still attached with the baffle, as figure(10). The other one is where the head of the mail is already pass through the baffle, as figure(11).

$$\theta_b = \begin{cases} tan^{-1}\left(\frac{y_0}{x_0}\right), if\ a \le h_b \\ \begin{cases} x^2 + y^2 = h_b^2 \\ \cos(\theta_m)\, y_0 - \sin(\theta_m)\, x_0 + \sin(\theta_m)\, x_b - \cos(\theta_m)\, y_b \end{cases} , if\ a > h_b \end{cases} \tag{9}$$

The normal force F_n and tangent force F_t baffle applies to mail is determined by geometric relation:

$$F_n = f_n \cos(90 - \theta_m - \theta_b) - f_p \sin(90 - \theta_m - \theta_b) \quad (10)$$

$$F_t = f_p \cos(90 - \theta_m - \theta_b) + f_n \sin(90 - \theta_m - \theta_b) \quad (11)$$

Mechanics of Materials

Refer to the mechanics of materials, we assume a paper as a rectangular beam. By applying the maximum shear stress formula of rectangular beam section, we can get the shear stress at y_1:

$$\tau = \frac{V}{2I}\left(\frac{h^2}{4} - y_1^2\right) \quad (12)$$

$$I_{rect} = \frac{1}{12}bh^3 \quad (13)$$

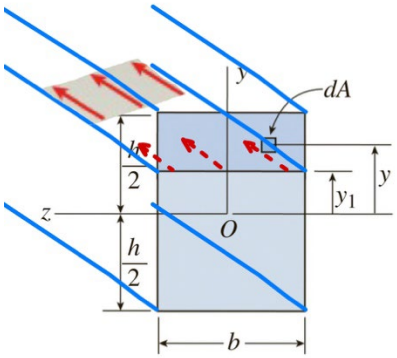

Figure (12). Shear stress for rectangular beam

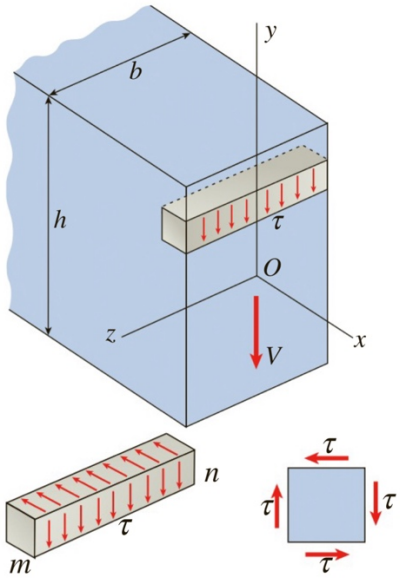

Figure (13). Shear stress at cross section

The maximum shear stress will be generated at neutral axis ($y_1 = 0$):

$$\tau_{max} = \frac{3V}{2A} \quad (14)$$

where the shear force is the normal force F_n baffle applies to mail:

$$V = F_n \quad (15)$$

On the other hand, the non-inclined stress is determined by the tangent force F_t baffle applies to mail:

$$\sigma = \frac{F_t}{A} \tag{16}$$

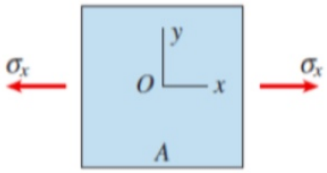

Figure (14). Non-inclined stress schematic

Finally, the total stress of the mail will be:

$$\sigma_{total} = \sigma + \tau_{max} \tag{17}$$

The deformation of the paper can eventually be calculated by apply the formula used in [1], where n = 0.58 is derived from figure (8).

$$\varepsilon = \frac{\sigma_{total}}{E_1} + \left(\frac{\sigma_{total}}{E_0}\right)^{0.58} \tag{18}$$

Bezier Curve

We choose cubic Bezier curve as the basis of our delivery path for some reasons:

1. Bezier curve is intended to approximate a real-world shape whose representation is unknown or too complicated and is often chosen to simulate the "Path".
2. It generates smooth, continuous curve by discrete points. Which is a great way to simplify the generation of the path.
3. Quadratic Bezier curve has only one concave direction, which may be too simple and cannot simulate the delivery action. Higher dimension Bezier curve can generate a more precise curve, but it will require more computation and time during the optimization. Hence, cubic Bezier curve is selected as the result of the tradeoff between complexity and precision.

A cubic Bezier curve is a curve of degree 3 and is defined by 4 points (P_0, P_1, P_2 and P_3). The curve starts at P_0 and stops at P_3. The line $\overrightarrow{P_0P_1}$ is the tangent of the curve in point P_0. And so it is the line $\overrightarrow{P_2P_3}$ in point P_3. In general, the curve will not pass through P_1 or P_2; the only function of these points is providing directional information. The distance between P_0 and P_1 determines "how long" the curve moves into direction P_1 before turning towards P_3.

The formula of the cubic Bezier curve:

$$B(t) = (1-t)^3P_0 + 3(1-t)^2tP_1 + 3(1-t)t^2P_2 + t^3P_3, 0 \le t \le 1 \tag{19}$$

schema of the curve is as below:

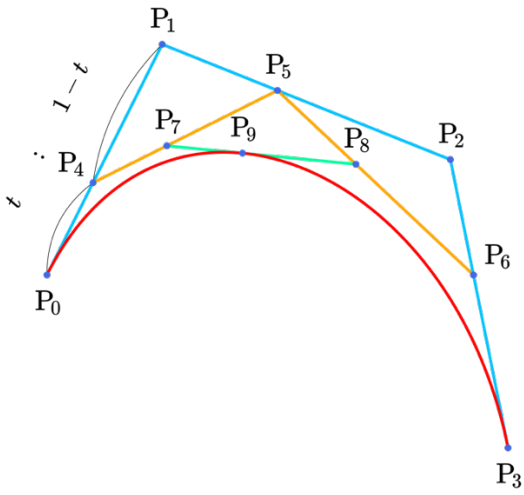

Figure (15). Bezier curve schematic

IV. Proposed Approach

Considering that the path before the mail touches the baffle will not cause deformation, our start point is set in front of the baffle. To observe the effect of the starting point, we alter its position in negative y direction between different tests. The end point is set at (-0.1, -0.017) where the head of the mail touches the back end of the mailbox, we assume the gripper can finish its task at there. The other two points P_1, P_2 will be chosen as the variable to optimize the result, or say to minimize the average deformation during the whole delivery.

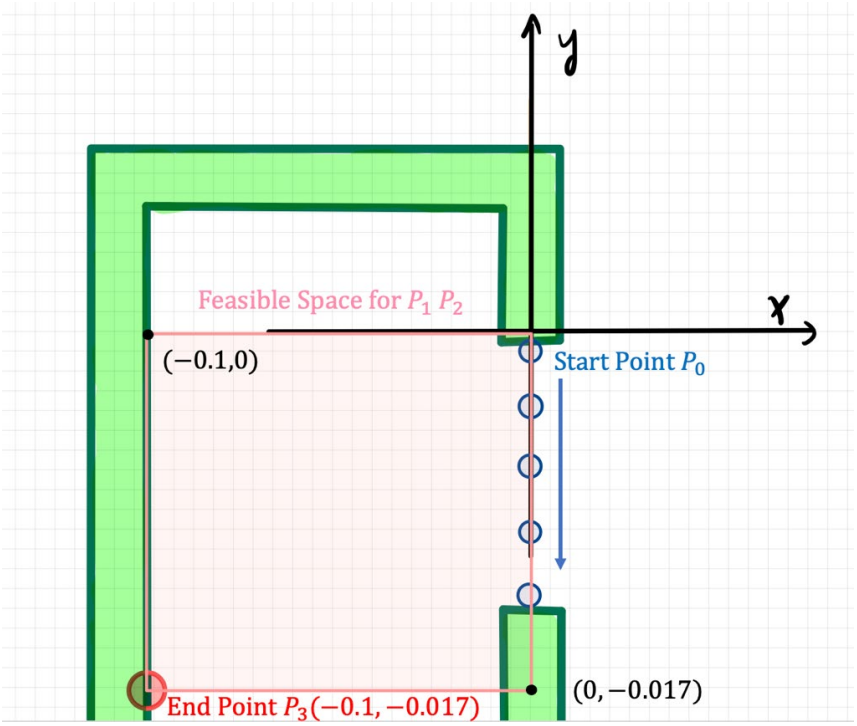

Figure (16). Testing Scenario

To calculate deformation, we need to select sample points on the Bezier curve, the point on the curve will represent the position of the head of the mail, and the mail is assumed to be tangential to the curve at the selected point.

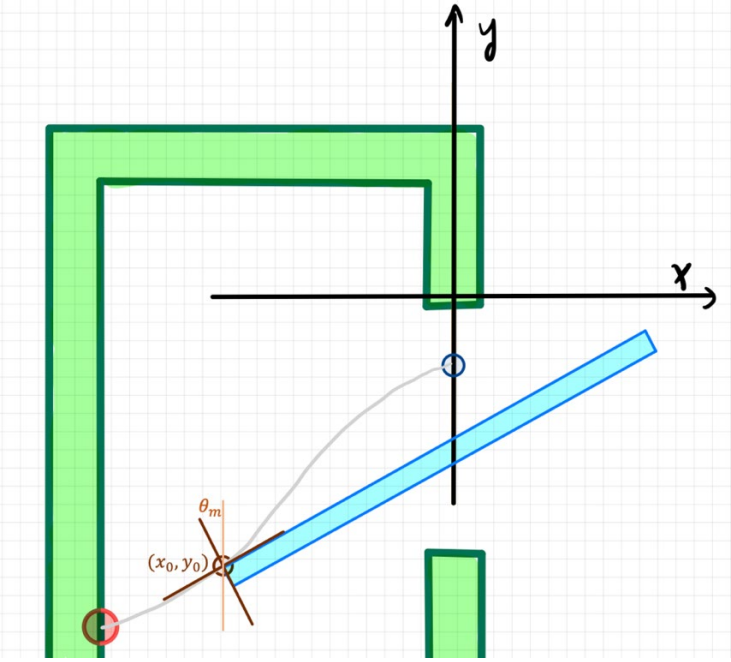

Figure (17). Bezier curve correspond to mail location

Constraints

Since we assume the mail is delivered downward in the end of the delivery, P_1 must be at the upper right of P_2.

$$P_2.x \leq P_1.x \tag{20}$$

$$P_2.y \leq P_1.y \tag{21}$$

The possible position for P_1 and P_2 are in the rectangular region enclosed by baffle and assumed end point P_3, as figure (16).

$$-0.1 \leq P_1.x \leq 0 \tag{22}$$

$$-0.017 \leq P_1.y \leq 0 \tag{23}$$

$$-0.1 \leq P_2.x \leq 0 \tag{24}$$

$$-0.017 \leq P_2.y \leq 0 \tag{25}$$

We restrict θ_m within the acceptable negative range, this is because we want to prevent the path from going upward. However, this constraint is based on the consideration of human behavior, it is a soft constraint and can be removed.

$$-9 \leq \theta_m(i) \leq 90° \,, 1 < i < N_b \tag{26}$$

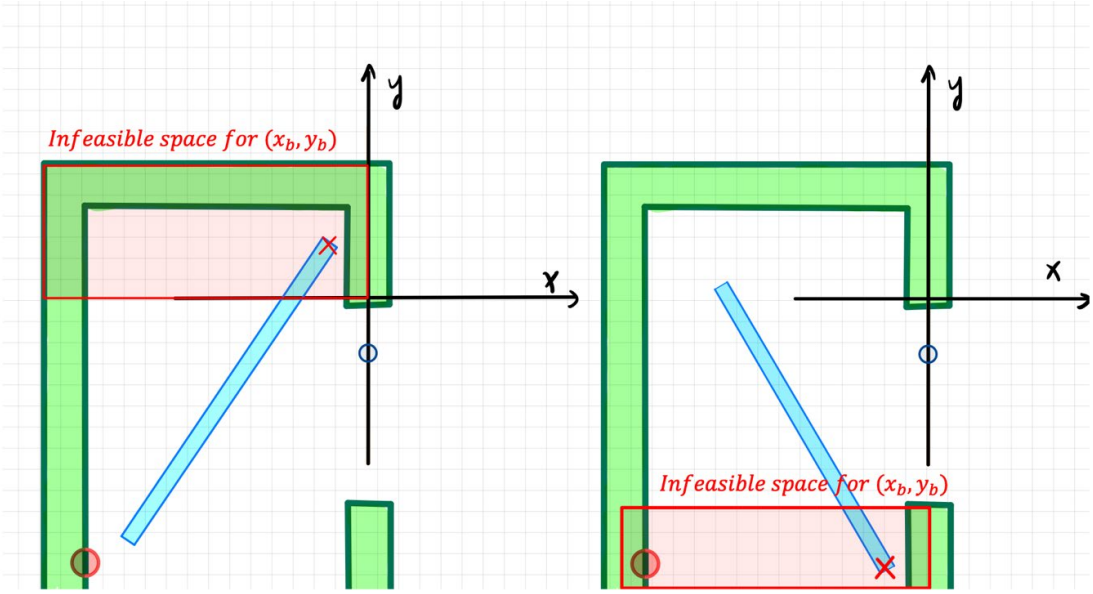

Figure (18). Infeasible space for (x_b, y_b)

During the delivery, the gripper position (x_b, y_b) should not be in the mailbox, hence there should be infeasible space for (x_b, y_b), as figure (18).

We refer to the idea in simulated annealing, when (x_b, y_b) and $\theta_m(i)$ conflict the constraint, we give output ε_{avg} a high enough value (at least 1000 times) to penalize the conflict.

objective _Deflection.m

if(x_n <= 0 && y_n >=0 ||x_n <=0 && y_n<=-0.015|| theta_m(i)<(-pi/20) || theta_m(i)>pi/2)
epsilon(i) = 1000*n; % at least 1000 times penalty
else

Mathematical Standard Form

$$min\, f(x) = \varepsilon_{avg} = \frac{\sum_{i=1}^{N_b} \varepsilon_i}{N_b}\ , N_b = number\ of\ selected\ point\ on\ bezier\ curve$$

subject to

$$h_1(x) = f_n - \frac{k*\theta_b + 0.5*mgh_b sin\theta_b}{a} = 0$$

$$h_2(x) = f_p - \mu * f_n = 0$$

$$h_3(x) = F_n - f_n\, cos(90 - \theta_m - \theta_b) + f_p\, sin(90 - \theta_m - \theta_b) = 0$$

$$h_4(x) = F_t - f_p\, cos(90 - \theta_m - \theta_b) - f_n\, sin(90 - \theta_m - \theta_b) = 0$$

$$h_5(x) = \sigma_{total} - \frac{F_t}{A} - \frac{3F_n}{2A} = 0$$

$$h_6(x) = \varepsilon - \frac{\sigma_{total}}{E_1} - \left(\frac{\sigma_{total}}{E_0}\right)^{0.58} = 0$$

$g_1(x) = P_2.x - P_1.x \leq 0$
$g_2(x) = P_2.y - P_1.y \leq 0$
$g_3(x) = P_1.x \leq 0$
$g_4(x) = -0.1 - P_1.x \leq 0$
$g_5(x) = P_1.y \leq 0$
$g_6(x) = -0.017 - P_1.y \leq 0$
$g_7(x) = P_2.x \leq 0$
$g_8(x) = -0.1 - P_2.x \leq 0$
$g_9(x) = P_2.y \leq 0$
$g_{10}(x) = -0.017 - P_2.y \leq 0$

since the feasible space for P_1 and P_2 are well-restricted, we can conclude that this problem is well-bounded.

Algorithm Selection

Since our problem is a to find an optimum path with minimum average strain, gradient-based algorithms or non-gradient-based algorithms can both be applied. In our case, we finally select fmincon but not GA, the reason is shown below.

1. For fmincon, the initial conditions can be easily set and close to the optimum because the size of mailbox is small. The x coordinate and y coordinate can only vary between [-0.1, 0] and [-0.017, 0].
2. Since we have five variables input for the optimization, using GA will spend too many times on selecting and mutating between variables. When we actually applied GA to solve the problem, it could no give us an answer after half an hour, but the same problem can be solved in 20 minutes by using fmincon.

Flowchart

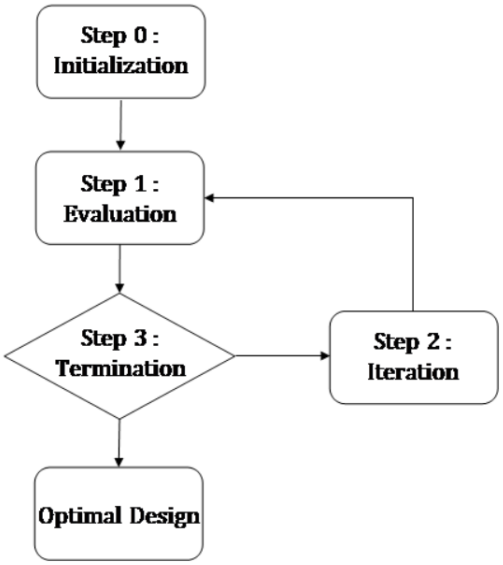

Figure (19). Flow chart

Step 0:

Set parameters, initial point p_0, end point p_3, the number of mails N, number of sample points for Bezier curve N_b

Step 1:

Set constraints and find other two points by fmincon to determine a Bezier curve. Cut the Bezier curve into n sample points and evaluate mean strains.

Step 2:

If the size of the current step is not less than the value of the step size tolerance and constraints are not satisfied to within the value of the constraint tolerance, go to the next iteration.

Step 3:

Iteration stops when the objective function is non-decreasing in feasible directions, to within the value of the optimality tolerance, and constraints are satisfied to within the value of the constraint tolerance. (By fmincon optimization stopping criteria)

Pseudo-code

Pseudo Code $(\boldsymbol{main.m})$
1: $\triangleright$ $p1x \in R$ *is the x coordinate of initial point*
2: $\triangleright$ $p4x, p4y \in R$ *are the coordinates of end point*
3: $\triangleright$ $n \in N$ *is number of sample points*
4: $\triangleright$ $x\_0 \in R$ *is starting points for fmincon*
5: $p1y \leftarrow p1y\_0$

6. $fmincon$ ($\boldsymbol{objective\_Deflection}, p1y, n$)
7. $return\ avg(\epsilon)$

Pseudo Code (**objective_Deflection.m**) (**p**)

1: ▷ $p \leftarrow [p1x, p1y, p2x, p2y, p0y]$
2: ▷ $n \in N$ *is number of sample points*
3: ▷ $[b_x, b_y, \theta_m] =$ **bezier**$(p0x, p0y, p1x, p1y, p2x, p2y, p3x, p3y, n)$
4: **for** *each* b_x, b_y, θ_m **do**
5: *Calculate* (x_b, y_b) ▷ *Coordinates of gripper*
6: **if** $(x_b \leq 0$ && $y_b \geq 0)$ **then**
7: $\epsilon = 100 * n$ ▷ *Infeasible penalty*
8: **else**
9: **cal_Deflection**(b_x, b_y, θ_m) ▷ *get* ϵ
10: **end if**
11: **end for**
12: $return\ avg(\epsilon)$

Pseudo Code (**bezier.m**) (**p0x, p0y, p1x, p1y, p2x, p2y, p3x, p3y, n**)

1: ▷ $p0x, p0y, p1x, p1y, p2x, p2y, p3x, p3y$ *are coordinates of points*
2: ▷ $n \in N$ *is number of sample points*
3: $t \leftarrow$ *devide* $[0, n]$ *into* $n + 1$ *points*
4: $b_x \leftarrow (1-t)^3 * p0x + 3 * (1-t)^2 * t * p1x + 3 * (1-t) * t^2 * p2x + t^3 * p3x$
5: $b_y \leftarrow (1-t)^3 * p0y + 3 * (1-t)^2 * t * p1y + 3 * (1-t) * t^2 * p2y + t^3 * p3y$
6: *Calculate* $\theta_m(b_x, b_y)$
7: *return* b_x, b_y, θ_m

Pseudo Code(**cal_Deflection.m**) (**b_x, b_y, θ_m**)

1: $a \leftarrow sqrt(b_x^2 + b_y^2)$ ▷ *distance from* (0,0) *to contact point*
2: **if** $a < h_b$
3: $\theta_b \leftarrow -atan2(y0, x0) - \pi;$
4: **else**
5: $a \leftarrow h_b$
6: *find the coordinate of the contact point*
7: *Calculate* $theta_b$ *from the contact point*
8: **end if**
9: *Calculate* $fn, fp, F_t, F_n, \tau, \sigma$
10: *Calculate* ϵ
11: return ϵ

V. Results

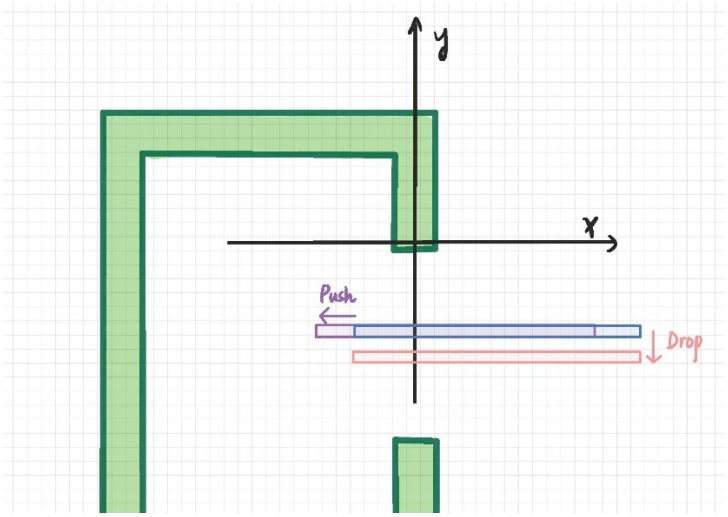

Figure (20). Schematic diagram of push and drop

In our results, we found that there's two types of motion in the delivered path, 'push' and 'drop', so we would like to define these two terms first.

1. When the delivered path is perpendicular to the baffle surface, we say that the mail is 'pushing' the baffle. For pushing, the mail will receive stress into the cross-section area
2. When the delivered path is tangent to the baffle surface, we say that the mail is 'dropping'. For dropping, the mail will receive shear stress perpendicular to the mail surface.

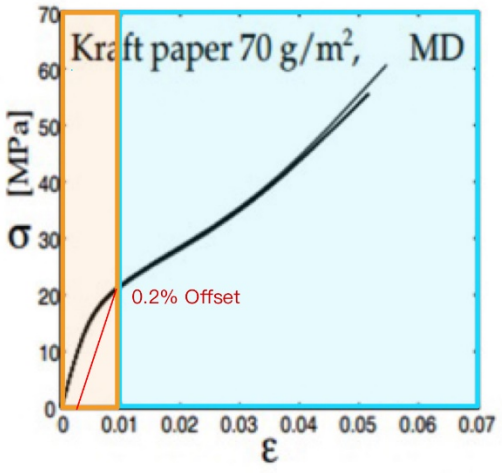

Figure (21). Region of elastic deformation and plastic deformation

Figure (21) shows the region of elastic deformation and plastic deformation. The elastic deformation region is defined by 0.2% strain offset.

Influence of variables

Our results show delivered paths with different initial points and the mean strain of each path. Since we set a penalty to constrain the angle of the gripper, if the mean strain is extremely big (bigger than 1), the path violates the angle constraint and do not have a feasible path.

1. Thickness of the mail bigger, the mean strain smaller and path 'push' more.

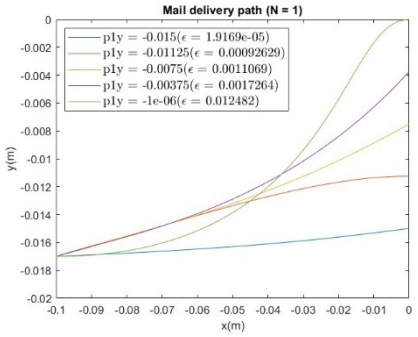	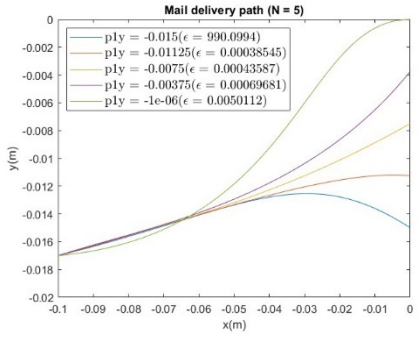	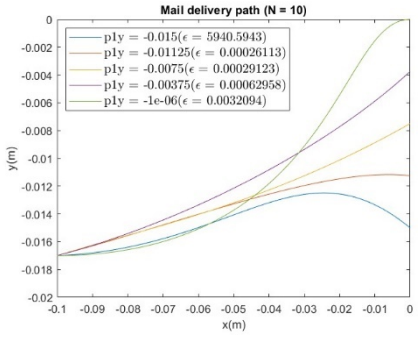
N = 1	N=5	N=10

Figure (22). Optimum path with different N

Figure (22) shows the optimum path with different N. We can find out that when the mail stack is thicker, the optimum path shows a higher preference of 'pushing'. Also, for the path start from the top of baffle with N = 1, the average strain is bigger than 0.01, which means the mail will suffer plastic deformation.

2. Friction coefficient higher, the paths prefer to 'push' the baffle.

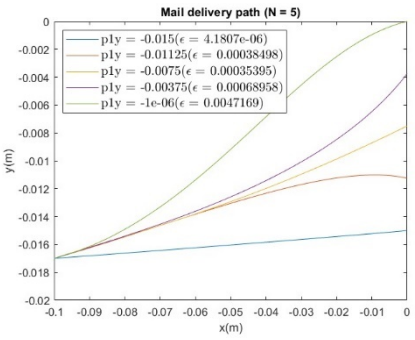	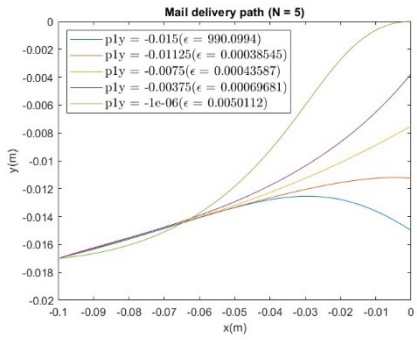
$\mu = 0.2$	$\mu = 0.4$

Figure (23). Optimum path with different friction coefficient

Figure (23) shows the optimum path with different friction coefficient. When the friction coefficient is higher, the optimize path will 'push' more to avoid deflection cause by friction force.

3. Spring constant bigger, the mean strain is higher.

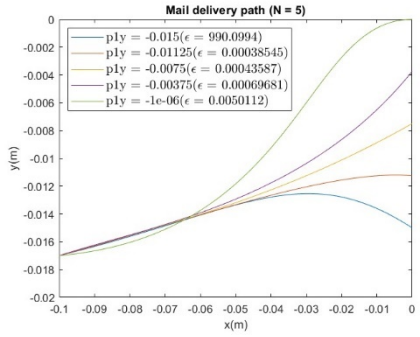	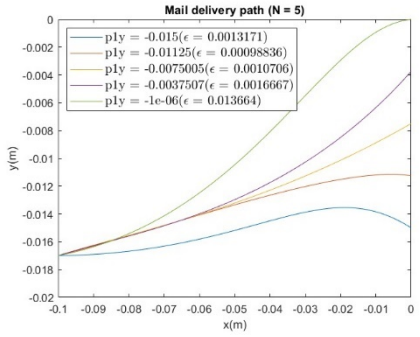
k = 0.0289 Nm	k = 0.289 Nm

Figure (24). Optimum path with different spring constant

Figure (24) shows the optimum path with different spring constant. The baffle is hard to push when the spring constant is big, so the path will avoid pushing the baffle and the average strain will become higher.

Active constraints and observations

Active constraints relaxation - θ_m

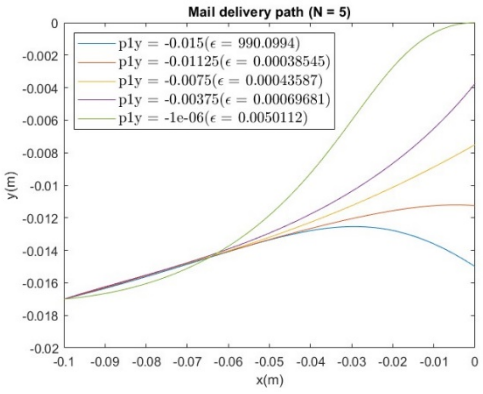	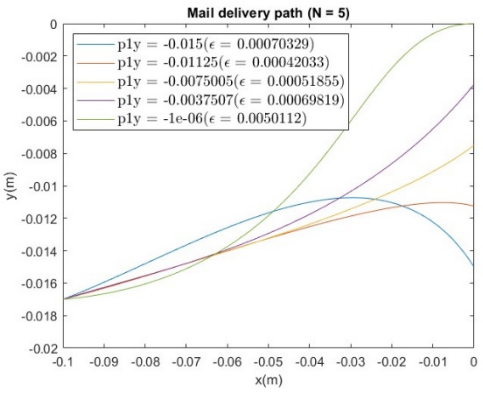
With θ_m constraint	Without θ_m constraint

Figure (25). Optimum path with soft constraint relaxation

By relaxing the soft constraint, we can see that the path starts from the bottom 'push' the baffle more.

Observations

1) Initial point:

   If the initial point is closer to the rotating shaft, the final average strain will be larger. Since a torsional spring is applied at the rotating shaft, to rotate the baffle at the same angle, it required more force if the force arm is shorter, which will lead to a bigger strain.

2) Thickness of the mail stack:
   The thicker the stack is, the mean strain will is smaller with the same initial point. The stress and shear stress will become smaller since the cross-section area becomes larger. When the stress is smaller, the mail will have a higher tendency to 'push' the baffle than 'drop' to get an optimize delivered path. Because we set the constraint on the turning angle of the gripper (θ_m), we give a penalty value when the constraint is violated. For the result, we can see that there are some extremely large values for the lowest path, which means that this path violated the constraint at some point on the curve.
3) Friction coefficient:
   When the friction coefficient is bigger, the gripper will have a tendency to 'push' the baffle first. Since the friction force is the product of normal force and friction coefficient, pushing the baffle can decrease the component force in the direction of the normal force to avoid extra friction force.
4) Torsional spring constant
   From the result, we can see that the gripper will have less tendency to push the baffle when the spring constant is bigger, which makes each path looks lower with the same initial point.

Verification

Fmincon algorithm provide a local minimum solution, hence with different initial point we might get a different solution set. However, if the average strain is within elastic deformation region, we assume the solution is acceptable. To observe how the initial point effect the solution, we choose another set of initial point. Figure (26) shows the result starting from different initial points without θ_m constraint.

<table>
<tr>
<td> 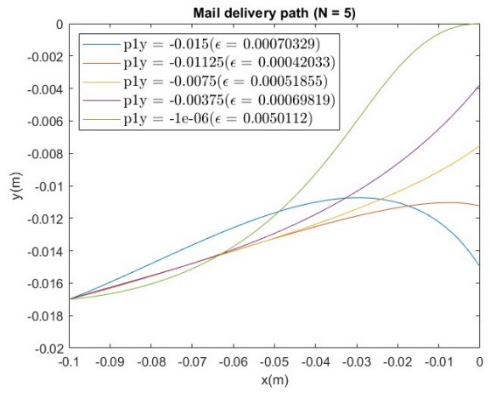
</td>
<td> 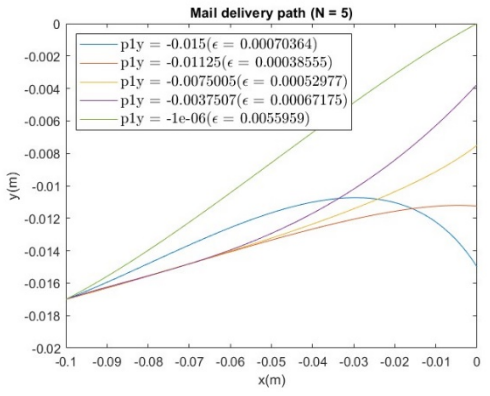
</td>
</tr>
<tr>
<td>Initial point
(p1x, p1y, p2x, p2y) = (0,0,0,0)</td>
<td>Initial point
(p1x, p1y, p2x, p2y) = (0,0, -0.1, -0.017)</td>
</tr>
</table>

Figure (26). Optimum path with different initial point

From figure (26), we can observe that the local minimum paths fmincon provide have a little different, but the average strains do not have much difference. Some of the results are better while others are not, which are both local optimal solutions for the problem and the mean strain is all in the elastic deformation region.

VI. Reference

[1] Mäkelä, Petri, and Sören Östlund. "Orthotropic elastic–plastic material model for paper materials." International Journal of Solids and Structures 40, no. 21 (2003): 5599-5620.
[2] Tryding, Johan. "In-plane fracture of paper." Division of Structural Mechanics, Lund Institute of Technology (1996).
[3]https://www.momoshop.com.tw/goods/GoodsDetail.jsp?i_code=7288441&osm=Ad07&utm_source=googleshop&utm_medium=traffic_pla&utm_content=bn&gclid=CjwKCAiAv9ucBhBXEiwA6N8nYMwHuEMCwCQCqtcq__3BIgEJIKMIUNe-5XU23h0Jckp4rMQtKJ6YPhoCsxcQAvD_BwE
[4] https://tw.misumi-ec.com/vona2/detail/110310556289/
[5] https://www.engineeringtoolbox.com/friction-coefficients-d_778.html

Source code (Github)

https://github.com/williampai0704/Mail_Delivery_Optimization.git